Anal. Chem. **2002,** *74,* 125−131

Determination of the Viscoelastic Properties of Polymer Films Using a Compensated Phase-Locked Oscillator Circuit

Seok-Won Lee and William D. Hinsberg[1]

Center for Polymer Interfaces and Macromolecular Assemblies, IBM Almaden Research Center, San Jose, California 95120

Kay K. Kanazawa

Department of Chemical Engineering, Stanford University, Stanford, California 94305

Using a combination of the quartz crystal microbalance and a corresponding physical model for the compound resonator, the viscoelastic properties of polymer films have been studied. By using a compensated phase-locked oscillator system, both resonant frequency and resistance (motional resistance of the Butterworth−Van Dyke equivalent circuit) can be measured simultaneously. The behavior of resistance as a function of film thickness or corresponding frequency shift provides a means not only for quantitatively determining the shear viscosity and elastic modulus of films but also for qualitatively comparing various systems. The physical model is extended to include four layers for describing dissolving/swelling films that form an energy-dissipative, interfacial layer. If the underlying film is rigid and acoustically thin, then the four-layer case can be reduced to a simplified three-layer description.

The quartz crystal microbalance (QCM) has emerged as a popular interface-monitoring technique due to its ability to perform real-time, rapid, and highly sensitive measurements of film thicknesses with angstrom resolution.[1−5] Impedance analysis of the quartz resonator can provide additional information on the solid/liquid interface including physical properties of the adjacent liquid and deposited film. This has been the subject of numerous theoretical studies.[6−12] The well-established Butterworth−van Dyke equivalent circuit has provided an excellent platform for relating electrical properties of the circuit to mechanical properties of deposited films. The equivalent circuit consists of two branches that represent the static (C_0) and motional characteristics (L, C, R) of the compound resonator, respectively (Figure 1a).[2] Among the four elements of the circuit, motional resistance (R) finds use in probing energy loss that occurs within the system, and the damping process is closely related to the physical properties of deposited films and adjacent liquid.[2,13]

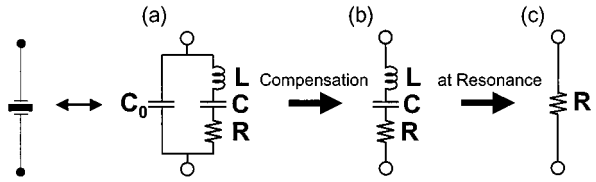

Figure 1. Representation of a quartz resonator: (a) Butterworth−Van Dyke equivalent circuit; (b) compensated circuit; (c) compensated circuit at resonance. At a resonant frequency, the inductive reactance ωL cancels the capacitive reactance $1/\omega C$, thereby leaving only R.

Compound quartz resonators have been modeled with two approaches. The first one is to represent the compound resonator as a Butterworth−Van Dyke equivalent circuit and to use a transmission line analogy to link the mechanical impedance to the electrical impedance in the motional arm.[7,14,15] The other approach is based on solving the wave equations and the piezoelectric constitutive equations that represent each layer (quartz, film, liquid).[6] Though this purely physics-based approach is less readily extended to multiple layers due to its complexity, the coupling of the physical properties of each layer provides an opportunity for examining the direct effects of the individual properties on frequency and electrical admittance.

The shunt capacitance C_0 results from the dielectric properties of the quartz disk and interconnection capacitances. The presence of this shunt capacitance distorts QCM data severely for lossy

* To whom correspondence should be addressed. E-mail: hnsbrg@almaden.ibm.com.

(1) Ward, M. D.; Buttry, D. A. *Science* **1990**, *249*, 1000−1007.
(2) Buttry, D. A.; Ward, M. D. *Chem Rev.* **1992**, *96*, 1355−1379.
(3) Fawcett, N. C.; Craven, R. D.; Zhang, P.; Evans, J. A. *Anal. Chem.* **1998**, *70*, 2876−2880.
(4) Niikura, K.; Matsuno, H.; Okahata, Y. *J. Am. Chem. Soc.* **1998**, *120*, 8537−8538.
(5) Patolsky, F.; Lichtenstein, A.; Willner, I. *J. Am. Chem. Soc.* **2000**, *122*, 418−419.
(6) Reed, C. E.; Kanazawa, K. K.; Kaufman, J. H. *J. Appl. Phys.* **1990**, *68*, 1993−2001.
(7) Martin, S. J.; Frye, G. C. *Ultrason. Symp. Proc.* **1991**, 393−398.
(8) Johannsmann, D.; Mathauer, K.; Wegner, G.; Knoll, W. *Phys. Rev. B* **1992**, *46*, 7808−7815.
(9) Kanazawa, K. K. *Faraday Discuss.* **1997**, *107*, 77−90.
(10) Martin, S. J.; Bandey, H. L.; Cernosek, R. W.; Hillman, A. R.; Brown, M. J. *Anal. Chem.* **2000**, *72*, 141−149.
(11) Etchenique, R.; Weisz, A. D. *J. Appl. Phys.* **1999**, *86*, 1994−2000.
(12) Hillman, A. R.; Jackson, A.; Martin, S. J. *Anal. Chem.* **2001**, *73*, 540−549.
(13) Nwankwo, E.; Durning, C. J. *Rev. Sci. Instrum.* **1998**, *69*, 2375−2384.
(14) Martin, S. J.; Gransaff, V. E.; Frye, G. C. *Anal. Chem.* **1991**, *63*, 2272−2281.
(15) Granstaff, V. E.; Martin, S. J. *J. Appl. Phys.* **1994**, *75*, 1319−1329.

10.1021/ac0108358 CCC: $22.00
Published on Web 11/30/2001

films by introducing a current whose phase shift is in quadrature with the applied voltage. This additional phase shift causes a change in both the magnitude and frequency at which the current to voltage phase shift is zero. The frequency of an oscillator of which the quartz serves as the frequency-determining element no longer is the series resonant frequency of the motional arm. Therefore, this shunt capacitance needs to be removed by a compensation method (Figure 1b).[16] At resonance, then, only R remains visible in the circuit since the inductive reactance ωL cancels the capacitive reactance $1/\omega C$ (Figure 1c), where ω is angular frequency. The precise measurement of resonance frequency by commercial instrumentation is usually performed by examining a spectral range in the neighborhood of a resonance frequency, using hundreds of measured data points and a computational fitting of these responses to an equivalent circuit model. Because of this, the detection of rapid, millisecond-time scale changes are difficult. Using the phase-locked approach, the oscillator remains locked on the resonance, permitting its continuous tracking.[16] The CPLO resonator system readily facilitates direct, undistorted real-time measurement of both resonance frequency and accompanying resistance at data rates that provide millisecond time resolution.[17]

This paper reports the behavior of resistance for materials and experimental conditions of relevance to the photoresist development process used in microlithographic imaging.[18] This paper also addresses the application of a physical model[6,9] to relate the resistance behavior to viscoelastic properties (shear viscosity η and elastic modulus μ) of polymer films. By itself, R is insufficient to determine both shear viscosity and elastic modulus, even when the thickness and density of a film are known, and multiple solutions are often possible;[12] therefore, further information is required. We will show in the present analysis that, by application of a detailed fitting procedure, the R behavior as a function of film thickness can be of use in illuminating the physical processes present during swelling or dissolution of thin polymer films.

THEORY

To make a quantitative assessment of the measurements taken using the compensated phase-locked oscillator during the polymer dissolution or swelling, it was necessary to extend the physical model[6,9] to include four layers.[17] This four-layer model is useful enough to describe most cases. These layers consist of the quartz, a viscoelastic polymer film, another viscoelastic layer that forms upon exposure to the liquid, and a final thick liquid layer. This analysis follows the spirit of that of Duncan−Hewitt and Thompson in their study of the structural interfaces formed when a QCM is interfaced to a liquid.[19] It is distinct from the analysis of the four-layer model given by Rodahl et al.,[20] which is based on a purely mechanical treatment of the four layers. In this report, we can only give the broadest outline of the path to the solution. The

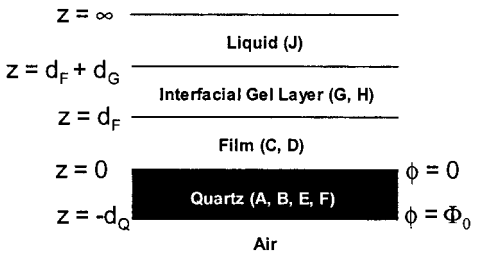

Figure 2. Geometry used for the analysis of the four-layer compound resonator. The interface between the quartz and the loaded film is set as the zero for the z axis. The d_G, d_F, and d_Q are the thicknesses of interfacial layer, film, and quartz, respectively. Φ_0 is the peak ac potential across the quartz.

geometry of the system considered is shown in Figure 2. The z axis is vertical and the shear motion takes place in a direction perpendicular to z. The z values on the left show the quartz thickness to be given by d_Q, the film thickness by d_F, and the gel thickness by d_G. The electric potentials are given by the values of zero at $z = 0$ and of Φ_0 at $z = -d_Q$. The constants indicated inside each layer represent values of parameters that are to be determined. A and B, C and D, G and H are the amplitudes of the waves traveling in the $-z$ and $+z$ directions, respectively. J is the amplitude of the shear wave in the liquid. E and F are constants describing the dielectric and piezoelectric fields in the quartz. These constants are all a function of frequency and the material properties of the media. The constant E takes on a special significance since the current density is expressed in terms of E through the relation

$$\mathscr{J} = -j\omega\epsilon_{22}E \qquad (1)$$

where ϵ_{22} is the appropriate dielectric constant for the AT-cut quartz and includes the frequency and the various material parameters. E is also proportional to the applied voltage Φ_0.

The constants are determined by the matching of boundary conditions at the interfaces shown in Figure 2. There are a total of nine boundary conditions at the four interfaces. These suffice to determine the nine constants. Table 1 presents the constitutive equations and solutions for each layer that result from this analysis.

Since the admittance $Y = \mathscr{J}/\Phi_0$, we can determine the admittance using eq 1. This admittance is very accurately represented by the equivalent circuit shown in Figure 1a. At the series resonant frequency, the inductive reactance ωL cancels the capacitive reactance $1/\omega C$. The losses in the resonator are characterized by the resistance R. The shunt capacitance C_P gives rise to a quadrature component of current. It adds a phase shift to the admittance, affecting the performance of phase-sensitive circuitry such as oscillators. In addition, the elimination of this capacitance makes the computation for the resonant frequency and resistance much simpler. When C_p is eliminated, then the resonant frequency is the frequency at zero phase, and the resistance is the reciprocal of the conductance at that frequency. To cancel the dielectric capacitance C_p in the theoretical analysis, we correct the admittance Y for the capacitance to give the admittance Y' for the series branch. C_P is given by the expression $C_P = j\omega\epsilon_{22}/d_Q$. Thus $Y' = Y - j\omega\epsilon_{22}/d_Q$. Using this expression,

(16) Brown, C. E.; Horne, D. E.; Frank, J.; Kanazawa, K. Meeting Abstracts, 194th Electrochemical Society **1998**, *98* (2), 1 .
(17) Hinsberg, W.; Lee, S.-W.; Ito, H.; Horne, D.; Kanazawa, K. *Proc. SPIE* **2001**, *4335*, 1.
(18) Hinsberg, W.; Wallraff, G.; Allen, R. In *Kirk-Othmer Encyclopedia of Chemical Technology*, 4th ed.; Kroschwitz, J., Ed.; Wiley-Interscience: New York, 1998; Supplement pp 233−280 .
(19) Duncan-Hewitt, W. C.; Thompson, M. *Anal. Chem.* **1992**, *64*, 94−105.
(20) Voinova, M. V.; Rodahl, M.; Jonson, M.; Kasemo, B. *Phys. Scr.* **1999**, *59*, 391−396.

Table 1. Constitutive Equations and Solutions for Each Layer[a]

layer	constitutive equations	solutions
liquid	$T_L = \eta_L \frac{\partial^2 u}{\partial z \partial t}, \quad \frac{\partial T_L}{\partial z} = \rho_L \frac{\partial^2 u}{\partial t^2}$	$u_L = (Je^{-ik_L z})e^{i\omega t}, \quad T_L = Jk_L\bar{\eta}_L Je^{-ik_L z}e^{i\omega t}$ where $k_L = \omega\sqrt{\frac{\rho_L}{i\omega\eta_L}}, \bar{\eta}_L = \eta_L\omega$
gel	$T_G = \mu_G \frac{\partial u}{\partial z} + \eta_G \frac{\partial^2 u}{\partial z \partial t}$ $\frac{\partial T_G}{\partial z} = \rho_G \frac{\partial^2 u}{\partial t^2}$	$u_G = (Ge^{ik_G z} + He^{-ik_G z})e^{i\omega t}, \quad T_G = ik_G\bar{\mu}_G(Ge^{ik_G z} - He^{-ik_G z})e^{i\omega t}$ where $k_G = \omega\sqrt{\frac{\rho_G}{\mu_G + i\omega\eta_G}}, \quad \bar{\mu}_G = \mu_G + i\omega\eta_G$
film	$T_F = \mu_F \frac{\partial u}{\partial z} + \eta_F \frac{\partial^2 u}{\partial z \partial t}$ $\frac{\partial T_F}{\partial z} = \rho_F \frac{\partial^2 u}{\partial t^2}$	$u_F = (Ce^{ik_F z} + De^{-ik_F z})e^{i\omega t}, \quad T_F = ik_F\bar{\mu}_F(Ce^{ik_F z} - De^{-ik_F z})e^{i\omega t}$ where $k_F = \omega\sqrt{\frac{\rho_F}{\mu_F + i\omega\eta_F}}, \quad \bar{\mu}_F = \mu_F + i\omega\eta_F$
quartz	$T_Q = c_{66}\frac{\partial u}{\partial z} + \eta_Q \frac{\partial^2 u}{\partial z \partial t} + e_{26}\frac{\partial \varphi}{\partial z}$ $D_Q = e_{26}\frac{\partial u}{\partial z} - \epsilon_{22}\frac{\partial \varphi}{\partial z}$ $\frac{\partial T_Q}{\partial z} = \rho_Q \frac{\partial^2 u}{\partial t^2}, \quad \frac{\partial D_Q}{\partial z} = 0$	$u_Q = (Ae^{ik_Q z} + Be^{-ik_Q z})e^{i\omega t}, \quad \varphi = \frac{e_{26}}{\epsilon_{22}}u + Ez + F,$ $T_Q = ik_Q\bar{\bar{c}}_{66}(Ae^{ik_Q z} - Be^{-ik_Q z})e^{i\omega t} + e_{26}E$ where $k_Q = \omega\sqrt{\frac{\rho_Q}{c_{66} + \frac{e_{26}^2}{\epsilon_{22}} + i\omega\eta_Q}}, \quad \bar{\bar{c}}_{66} = \epsilon_{22}c_{66} + e_{26}^2 + i\epsilon_{22}\omega\eta_Q$

boundary conditions: (1) $T_Q = 0$ at $y = -d_Q$;(2) $\varphi = \Phi_0$ at $y = -d_Q$; (3) $T_Q = T_F$ at $y = 0$; (4) $u_Q = u_F$ at $y = 0$; (5) $\varphi = 0$ at $y = 0$; (6) $T_F = T_G$ at $y = d_F$; 7) $u_F = u_G$ at $y = d_F$; (8) $T_G = T_L$ at $y = d_F + d_G$; (9) $u_G = u_L$ at $y = d_F + d_G$

[a] Definitions: T (stress), u (strain), D_Q (electric displacement vector for quartz), ρ (density), c_{66} (elastic shear modulus for quartz), e_{26} (piezoelectric constant for quartz), ϵ_{22} (dielectric constant for quartz), η (viscosity), and μ (elastic modulus).

we have used Mathcad software to create an algorithm to locate the frequency for zero phase of Y' and the value of the conductance at that frequency. We can determine the values for all of the constants (A, B, C, D, E, F, G, H, and J) but will not discuss these results here. When $d_G = 0$, the model describes a system that does not form an interfacial layer.

EXPERIMENTAL SECTION

Materials. Glycerol and aqueous 0.26 N tetramethylammonium hydroxide (TMAH) solution were obtained from EM Science (Gibbstown, NJ) and Shipley (Marlborough, MA), respectively. Propylene glycol methyl ether acetate (PGMEA) was obtained from Pacific PAC International (Hollister, CA) and used as casting solvent for a copolymer of norbornene carbonate (NBCarb) and norbornenecarboxylic acid (NBCA) (NBCarb/NBCA = 70/30; MW = 58 000).[21] This cycloolefin copolymer was available from a previous study.[21] Poly(*n*-butyl acrylate) (20 wt % solution in toluene; MW = 62 000) was obtained from Polysciences (Warrington, PA). Poly(styrene) (MW = 280 000) was obtained from Aldrich Chemical (Milwaukee, WI), and toluene (EM Science, Gibbstown, NJ) was used as its casting solvent.

Methods. For the preparation of thin films, polymers were dissolved in casting solvents and the prepared solutions were spin-coated at 3000 rpm for 1 min onto 5-MHz quartz crystal resonators (Maxtek Inc., Santa Fe Springs, CA). The coated films were then baked on a hot plate at 130 °C for 2 min and allowed to cool to room temperature. The physical thickness of films was measured using an Alpha-Step 200 profilometer (Tencor Instruments, San Jose, CA; estimated precision of 50 nm). Film thicknesses thus measured agreed to better than 5% with those values obtained using a Gaertner L116 ellipsometer (Gaertner Scientific Corp., Chicago, IL; estimated precision of 3 nm) for optical film thickness analysis. Film densities were estimated, using the Sauerbrey relation, from the crystal resonance frequency shifts in air induced by polymer films of known thickness <1000 nm. The density values thus obtained are consistent with literature values reported for the bulk polymers.[22]

The film-loaded quartz crystals were then mounted on a Maxtek KPS-550 sensor probe, used in conjunction with a HP 4334A Universal Counter (Hewlett-Packard, Palo Alto, CA) and an IBM PC. The instrumentation was controlled by a custom-made program using Labview software (National Instruments, Austin, TX). The CPLO circuit for the QCM setup is described in the literature.[23]

To characterize the effects of film thickness, the following procedure was used. A bare crystal was mounted in the probe, and its frequency and resistance were noted. The probe was immersed in deionized water, and the changes in frequency and resistance were recorded. The same crystal was then coated with the polymer film of interest, and the film thickness after postapply bake was measured. The frequency and resistance of the coated

(21) Ito, H.; Allen, R.; Opitz, J.; Wallow, T.; Truong, H.; Hofer, D.; Varanasi, P.; Jordhamo, G.; Jayaraman, S.; Vicari, R. *Proc. Photo-Opt. Instrum. Eng.* **2000**, *3999*, 2−12.

(22) Van Krevelen, D. *Properties of Polymers*, 2nd ed.; Elsevier: New York, 1972: p 70.

(23) Kanazawa, K. K.; Frank, J. The Electrochemical Society, Boston, 1998; No. 1210.

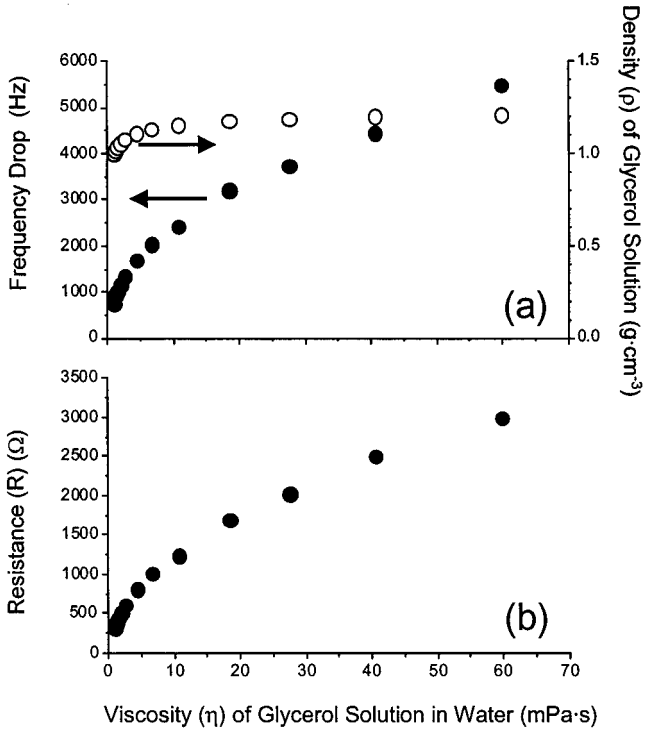

Figure 3. (a) Frequency drop (solid circle) and density (open circle) (b) resistance of aqueous glycerol solution as a function of viscosity.

crystal in air and the frequency and resistance shifts upon immersion in water were recorded as before. Repeated trials showed that the frequency shifts and resistance values attributable to film loading, and those attributable to immersion in water, were reproducible to better than 5%. Visible reflectance spectroscopy using an model PC2000 fiber-optic spectrometer (Ocean Optics Inc., Dunedin, FL) of poly(styrene) and poly(*n*-butyl acrylate) films confirmed that their thicknesses are unchanged following immersion in water.

RESULTS AND DISCUSSION

Dependence of Resistance and Frequency Shift on Liquid Viscosity. The shear oscillation of the quartz crystal in contact with liquid has been studied,[24,25] and the solution for the resonant frequency suggests that the frequency change also reflects the degree of energy dissipation that originates from the viscosity of the liquid. Therefore, it is of interest to investigate the effectiveness of resistance as an indicator of energy dissipation in comparison to resonant frequency. This was useful also to verify the capacitance correction and operation of the phase-locked oscillator. We prepared mixtures of glycerol ($\eta = 1499$ mPa·s at 20 °C) and water ($\eta = 1$ mPa·s at 20 °C) at various compositions (0−80 wt % glycerol). A bare quartz surface was immersed in each solution at room temperature (~20 °C) for the measurement of frequency shift and resistance. Figure 3 shows the data of the resonant frequency shift and resistance, which are subtracted from the values in air, with respect to liquid viscosity. The density and viscosity data are values at 20 °C. The solution density sharply increases from ~1.0 g·cm^{-3} as the viscosity increases and then

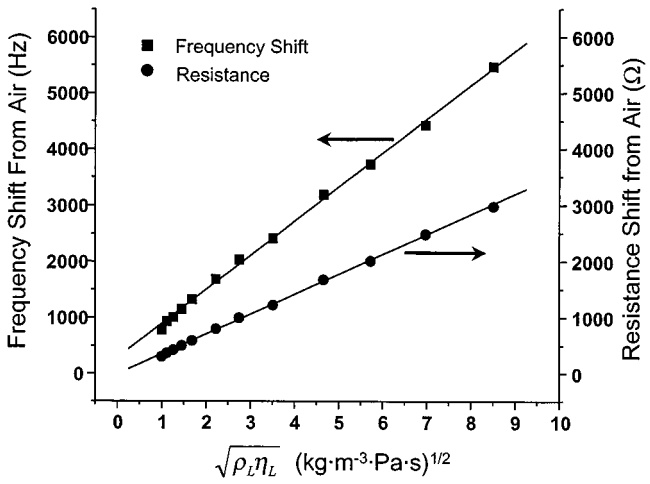

Figure 4. Correlation of $(\rho_L\eta_L)^{1/2}$ with frequency shift and resistance shift for water/glycerol mixtures. The values of frequency shift and resistance are calculated by subtracting the observed shift in value when immersed in the liquid to that when immersed in air. The solid lines are the linear least-squares fits to the data; in both cases, the correlation coefficients *R* are greater than 0.999.

reaches a plateau of ~1.2 g·cm^{-3} at a viscosity of ~5−10 mPa·s. This initial sharp increase in density may explain the steeper rise of resonant frequency shift and resistance at the same viscosity range (zero to ~5 mPa·s). At liquid viscosities larger than ~5 mPa·s, where there is no significant change in liquid density, the further increase in resonant frequency and resistance may be attributed only to liquid viscosity.

To simultaneously compare resistance with frequency shift in response to the liquid properties (ρ_L and η_L), the data shown in Figure 3 are presented in Figure 4 as resonant frequency shifts and resistance shifts from the values in air with respect to $(\rho_L\eta_L)^{1/2}$ of the liquid. These data exhibit a linear dependence on $(\rho_L\eta_L)^{1/2}$, in agreement with the theory.[25,26] At a larger $(\rho_L\eta_L)^{1/2}$ (~8.5 kg$^{1/2}$·m$^{-2/3}$·Pa$^{1/2}$·s$^{1/2}$), resistance increases up to ~10 times that of pure water, while frequency shift increases up to ~7 times. The wide response range of resistance suggests that it can serve as a sensitive monitor of energy dissipation.

Effect of Film Thickness. The resistance of a compound resonator system may be described as a sum of contributions from each layer (quartz, film, fluid):

$$R = R_{\text{quartz}} + R_{\text{film}} + R_{\text{fluid}} \quad (2)$$

We can further simplify eq 2:

$$R = R_0 + R_{\text{film}} \quad (3)$$

where R_0 is resistance for the case where no film is present ($R_0 = R_{\text{quartz}} + R_{\text{fluid}}$). Experimentally, typical R_0 values in air and in water are ~11 and ~320 Ω, respectively. The contribution of a loaded film to the total resistance is not significant with rigid polymers such as polystyrene and poly(methyl methacrylate), whose glass transition temperatures are well above room temperature. For example, R_{film} for a 6000-nm-thick film of polystyrene

(24) Nomura, T.; Okuhara, M. *Anal. Chim. Acta* **1982**, *142*, 281−284.
(25) Kanazawa, K. K.; Gordon II, J. G. *Anal. Chem.* **1985**, *1985*, 1770−1771.
(26) Muramatsu, H.; Tamiya, E.; Karube, I. *Anal. Chem.* **1988**, *69*, 2142−2146.

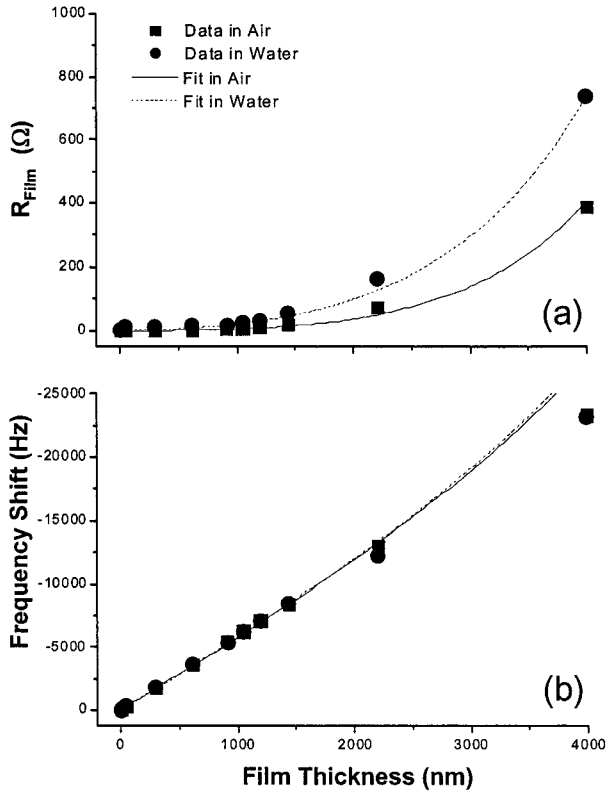

Figure 5. Resistance increase and frequency shift due to film loading in air and water. The data were obtained by subtracting values of bare quartz resonators from those of film-loaded ones. The solid and dashed lines are obtained from the physical model of three layers ($d_G = 0$) at $\mu = \sim 3 \times 10^7$ Pa and $\eta = \sim 0.13$ Pa·s.

($T_g = 100$ °C) is only ~11 Ω, approximately the value for a bare quartz resonator in air. However, rubbery polymers, whose glass transition temperatures are below room temperature, exhibit resistance behaviors that sharply contrast with those of rigid films. Figure 5a shows R_{film} behaviors of poly(*n*-butyl acrylate) (PBA) films ($T_g = -64$ °C) in air and water as a function of film thickness that are found to be typical of lossy polymers. The resistance initially does not show any significant increase and then begins to increase sharply with film thickness (~1500 nm for PBA). The shape and position of the curve serve well as a qualitative measure of viscoelastic properties of deposited polymeric films. A comparison of predictions of the physical model with experiment indicates that these resistance data are consistent with an elastic modulus (μ_F) of $\sim 3 \times 10^7$ Pa and shear viscosity (η_F) of ~0.13 Pa·s. It is notable that frequency shifts due to film loading that were measured in air and water are the same (Figure 5b). This means that the effect of film loading on resonance frequency is additive within the thickness range of interest here and the effect of the film/liquid interface on frequency shift is negligible, demonstrating that the shifts in resonant frequency are insensitive to the viscoelastic nature of the film. In contrast to frequency shift, the extent to which resistance due to film loading (R_{film}) changes with film thickness depends on whether the resonator is immersed in air or in water. We infer that this difference results from the interaction between film and viscous liquid layers, which is negligible at the air/film interface.

The physical model predicts this differing behavior in resistance. Figure 6 plots as discrete points the differences between

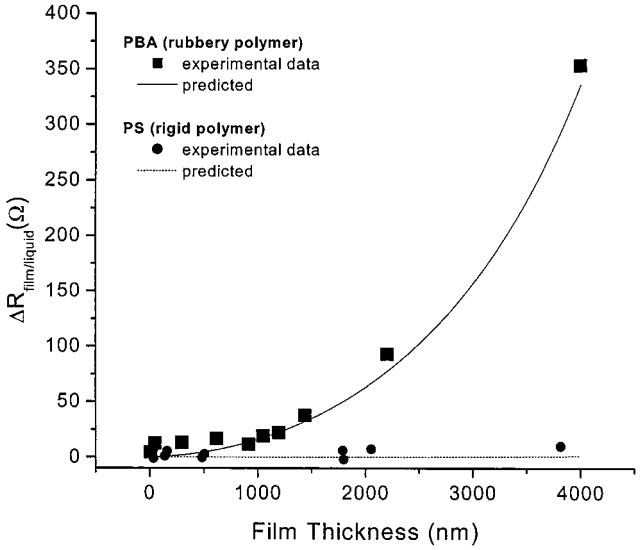

Figure 6. Contribution of the liquid/film interface to the total resistance as a function of film thickness.

measured values of R_{film} in air and R_{film} in water at different thicknesses for the PBA polymer films (derived from the data in Figure 5a) and for PS films. The purpose of this subtraction is to remove from the resistance value the contribution due to losses within the bulk of the polymer film and to thereby isolate the contribution due to the medium in which the films are immersed. The lines in Figure 6 represent the theoretical differences in resistance with respect to film thickness for the case of rubbery PBA (solid) and rigid polystyrene (PS) (dashed), predicted using the physical model. For PBA, the resistance difference increases as the distance of the liquid/film interface from the quartz surface increases. Presumably the larger distance between the quartz surface and liquid/film interface leads to increased interfacial displacement, thereby producing greater energy dissipation. In contrast to the behavior of rubbery PBA films, PS films exhibit negligible changes in the resistance R_{film} with thickness, whether immersed in air or in water. These observations suggest that resistance measurement can provide information not only of the intrinsic physical properties of films but also of the film surface in contact with liquid.

Effect of the Formation of an Interfacial Layer on Resistance. Formation of an interfacial "gel" layer at the liquid/film interface is common in many areas, where the polymer experiences plasticization by the penetration of solvent or solution.[27−30] In most cases, the interfacial layer is regarded to possess a gelatinous swollen structure due to the infusion of liquid. We have studied a copolymer of 70 mol % NBCarb and 30 mol % NBCA, the synthesis and properties of which are described elsewhere.[21] This copolymer P(NBCarb−NBCA) swells but does not dissolve in aqueous base, thereby providing a simple model system to investigate the effect of formation of an interfacial layer on resistance.

Figure 7a presents the resonant frequency and resistance behavior of a ~1600-nm-thick P(NBCarb-NBCA) film upon im-

(27) Narasimhan, B. *Adv. Drug Delivery Rev*, **2001**, *48*, 195−210.
(28) Rossi, G.; Mazich, K. *Phys. Rev. E* **1993**, *48*, 1182−1191.
(29) Herman, M.; Edwards, S. *Macromolecules* **1990**, *23*, 2662−3671.
(30) Narasimhan, B.; Peppas, N. *Adv. Polym. Sci.* **1997**, *128*, 157−207.

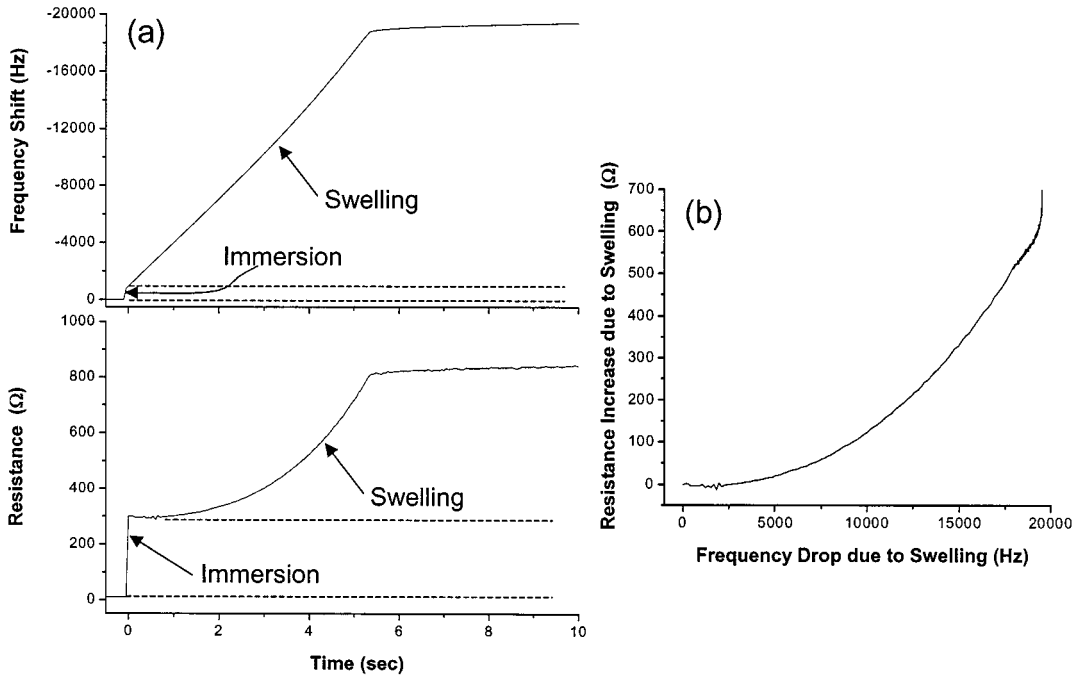

Figure 7. (a) QCM behavior in frequency shift and resistance of a 1600-nm-thick P(NBCarb-NBCA) polymer in 0.26 N TMAH solution and (b) resistance increase−frequency shift relationship due to swelling.

mersion into aqueous 0.26 N TMAH solution. Upon immersion, the frequency rapidly decreases by ∼800 Hz and resistance increases by ∼310 Ω, attributable to the presence of liquid. The P(NBCarb−NBCA) film exhibits a further decrease in frequency that follows the rapid initial ∼800-Hz frequency decrease and reaches a plateau at ∼5.5 s. The frequency decreases linearly with time. This suggests that the gel layer/dry film interface advances at a constant rate and that the permeation of solution into the film is governed by a non-Fickian process known as case II diffusion, where the rate of solvent diffusion is rapid compared to other processes (e.g., polymer relaxation or, in this case, chemical reaction) that alter the polymer structure.[31] Such a frequency decrease has been attributed to an increase in film mass due to permeation of the solution into the polymer film.[21,32] The apparent film mass has increased by nearly 175% at ∼5.5 s. Parallel behavior is seen in the resistance response. The expected resistance increase upon immersion is followed by a further nonlinear increase that coincides with the period of frequency decrease. At the point where the front of the interfacial layer reaches the quartz surface (at ∼5.5 s in Figure 7a), the rapid increase in resistance stops; the slight changes in resistance and frequency after that point are presumably due to further slow uptake of the solution. The swelling of the film here is promoted by a chemical reaction at the film/liquid interface, where base deprotonates acid groups pendant to the polymer chain. This leads to the formation of a polar ionic polymer structure that promotes penetration of the aqueous solution and further neutralization, thereby producing a gellike layer. Immersion of the same copolymer film into pure water does not lead to such significant changes in resistance and frequency. It was observed that, following immersion in water, the ∼1600-nm-thick film shows ∼300-Hz further decrease in frequency and ∼25 Ω further increase in resistance, which sharply contrasts with ∼18000 Hz and ∼500 Ω by immersion into the base solution.

The decrease in resonant frequency due to swelling in aqueous base, which represents the amount of solution uptake into the film, may be plotted with respect to the accompanying increase in resistance, as shown in Figure 7b. Assuming that resonant frequency changes are linearly related to the film thickness (as is the case with films of the rubbery polymer PBA for thicknesses up to 4000 nm as shown in Figure 5b) and that the composition of solution in the gel layer is uniform with depth, the frequency shift-resistance relationship can be used to understand the viscoelastic character of the interfacial layer. By comparing predictions of the physical model with the frequency shift−resistance data, the experimental data are consistent with the formation and growth of an interfacial layer with an elastic modulus (η_F) of ∼4 × 10^7 Pa and shear viscosity (μ_F) of ∼0.13 Pa·s, which indicates that the gel layer approximately possesses a viscoelastic character of rubbery PBA. This suggests that such film thickness−resistance plots have utility as a method to estimate the physical properties of unknown organic films for comparison with those of well-understood polymers such as PBA.

CONCLUSION

We have demonstrated that the simultaneous measurement of resonant frequency and resistance, which can be carried out at high data acquisition rates, provides information to better understand the viscoelastic properties of polymer films. In particular, resistance values isolated from the Butterworth−Van Dyke circuit by our compensated phase-locked oscillator (CPLO)

(31) Crank, J. *The Mathematics of Diffusion*, 2nd ed.; Oxford Science Publications: New York, 1975; Chapter 11.
(32) Toriumi, M.; Ohfuji, T.; Endo, M.; Morimoto, H. *J. Photopolym. Sci. Techonol. Jpn.* **1999**, *12*, 545−551.

system have shown their utility as an indicator of the energy-dissipating character of the compound resonator system. The system is also found to be useful for better understanding the formation and physical properties of interfacial, gelatinous layers. A four-layer physical model has been used for comparison with experimental data and extraction of viscoelastic parameters, and the resistance behavior with respect to film thickness or frequency shift is found to serve well as a qualitative measure of viscoelastic properties of deposited polymeric films. The contribution of dry, rigid films at thicknesses less than $\sim 2\ \mu$m to total resistance has been found to be negligible, so for this special case, the three-layer physical model produces results almost identical to those for the four-layer model.

ACKNOWLEDGMENT

This research was supported by NSF Materials Science and Engineering Research Center Grant 9808677 to the Center for Polymer Interfaces and Macromolecular Assemblies at Stanford University. The authors express sincere thanks to Dr. Don E. Horne at IBM for his help with the phase-locked oscillator QCM circuit. S.-W.L. also thanks Drs. Thomas I. Wallow, Youngjoon Lee, and Hiroshi Ito at IBM for discussions on polymer synthesis and characterization.

Received for review July 24, 2001. Accepted October 22, 2001.

AC0108358